A reassessment of the strain model of superconductivity and a search for a Kosterlitz-Thouless Transition in $BaFe_2As_2$

Tim Blasius

Physics Department, University of Michigan
May 2010
Thesis Chair: Professor Kurdak
Research Advisor: Professor Stewart (University of Florida)

Abstract

Superconducting crystals of the compound $BaFe_2As_2$, which is a member of the recently discovered class of "122 structure" iron-arsenic superconductors, MFe_2As_2, were made. Our group was the first to observe a complete superconducting resistive transition in the undoped compound $BaFe_2As_2$ ($T_c^{onset} = 22.5K$). The resistive transition was measured before and after annealing one of the crystals. No disappearance of the superconducting state after annealing was noticed (in fact the transition became sharper), which does not verify the standing idea that crystallographic strain is the source of superconductivity in undoped MFe_2As_2. The current sensitivity of the resistive transition, the lack of a diamagnetic signal in magnetic susceptibility measurements, the superconducting state's sensitivity to the removal of crystallographic layers, and upper critical field anisotropy consistent with the anisotropy of the crystal lattice, lead to the belief that the $BaFe_2As_2$ crystals are not bulk superconductors. Rather, it is inferred that the superconductive state is filamentary or more probably planar in nature. This evidence led to a search for a Kosterlitz-Thouless transition, which is known to exist in 2D superconductors. Three methods were used to probe for the presence of a Kosterlitz-Thouless transition, two of which yielded consistent answers for the transition temperature T_{KT}. From this it is believed that evidence of a Kosterlitz-Thouless transition and hence two-dimensional superconductivity has been found in $BaFe_2As_2$.

Basic Introduction to Superconductivity:

Heike Kamerlingh Onnes successfully liquefied helium in 1908. Shortly thereafter, in 1911, he discovered that the pure metal mercury exhibits zero resistance when subjected to liquid helium temperatures. He had discovered a new state of matter – superconductivity.

It took nearly half a century until Bardeen, Cooper, and Schrieffer (BCS) finally gave the scientific community a microscopic theory of superconductivity. They found that electrons could form bound pairs by exchanging phonons in a material's lattice. That is, even though we think of electrons as intrinsically repelling one another, in the medium of a crystal lattice there can exist an attractive interaction. Qualitatively the process is as follows, as one electron travels though the lattice it will distort the positions of the positively charged lattice around it, creating a higher density of positive charge in its wake. This more densely packed region will then pull a trailing electron towards it and the two electrons can carry on in this fashion and are thus bound together with the lattice as a medium. This situation is displayed in fig. 1.

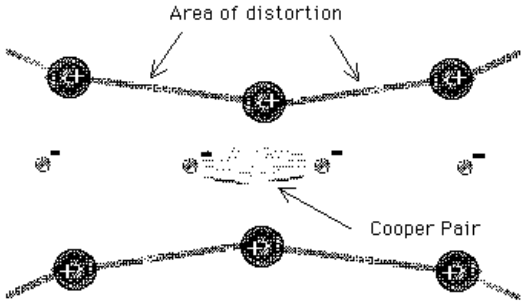

Fig. 1: Cartoon of a cooper pair. [1].

BCS theory provides a beautiful explanation for superconductivity in many simple compounds. However, BCS theory does not accurately describe the forms of superconductivity found in most compounds of current interest (including those studied in this paper). BCS theory provides an interesting qualitative picture but it is not strictly correct for our compound and, therefore, we are better served by a phenomenological description.

Meissner discovered that the lack of electrical resistance was not the only hallmark of the superconducting state. A superconductor (type I) also completely expels magnetic fields. Do not mistake the significance of this statement. This does not only mean that induction currents perfectly prevent changes in magnetic field, but that static magnetic fields will be expelled as well.

These two physical phenomena, lossless conduction of electrons and the expulsion of a magnetic field (Meissner Effect), are described by the London Equations. [2]

$$\vec{E} = \frac{\partial}{\partial t}\left(\Lambda \vec{J}_s\right) \tag{1}$$

$$\vec{B} = -c \cdot \nabla \times \Lambda \vec{J}_s \tag{2}$$

$$\Lambda = \frac{4\pi\lambda^2}{c^2} = \frac{m^2}{n_s e^2} \tag{3}$$

Eq. 1 describes perfect conductivity. It states that an applied electric field will continually accelerate superconducting charges and that superconducting charges will move at constant velocity in the absence of an electric field. This is in stark contrast to Ohm's law. Eq. 2, when paired with Ampère's law, yields eq. 4 [2]:

$$\nabla^2 \vec{B} = \frac{\vec{B}}{\lambda^2} \tag{4}$$

This equation implies that magnetic fields are exponentially screened from the bulk of the superconductor, which is a restatement of the Meissner Effect.

The expulsion of a magnetic field from a superconductor costs energy. We can recall from introductory E/M theory that the energy stored in a magnetic field is as shown in eq. 5.

$$\int \frac{B^2}{2\mu_0} dVol \tag{5}$$

The expulsion of a magnetic field is the same as the creation of a magnetic field of equal magnitude and opposite orientation. Thus, the application of a magnetic field can easily make the superconducting state energetically unfavorable. That is, the energy gained by entrance into the superconducting state can be overcome by the energy needed to generate a magnetic field. Type I superconductors have an upper critical field, H_c, which signifies the largest magnetic field to which a sample may be subjected without completely exiting the superconducting state.

Type II superconductors are able to remain superconducting in much higher applied fields. This is possible because, instead of totally expelling an applied magnetic field, they allow it to penetrate in quantized flux vortices. Type II superconductors have two critical fields: H_{c1} and H_{c2}. At a field of magnitude H_{c1}, magnetic vortices begin to form, and at a field magnitude of H_{c2} superconductivity is completely destroyed. A cartoon of magnetic flux vortices penetrating through a sample is shown in fig. 2. The magnetic field in flux vortices destroys superconductivity inside them, but the regions between flux vortices retain the superconducting state.

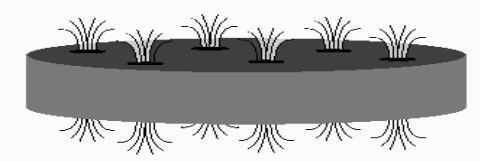

Fig 2. A cartoon of magnetic flux vortices penetrating a cylindrical superconductor [2].

While formation of magnetic flux vortices may allow the superconducting state to persist at higher applied fields, they can also plot the course of its destruction. If transport currents are passed through a type II superconductor, they will impart a force upon the magnetic flux vortices. If there are no other forces acting on the vortices (e.g. forces from the crystal lattice), then the currents will move them. This causes energy loss, which can be interpreted as a finite resistance. Thus the vortex state can cause a type II superconductor to exhibit a finite resistance. This fact will become crucially important when we discuss Kosterlitz-Thouless transitions later.

Experimental Technique: Sample Preparation

Before we can test theory, we must grow the crystals we wish to study. We do this by dissolving at high temperature the correct molar amounts of the elements needed for the crystal into a metal flux. Then we slowly lower the temperature until super-saturation is reached and the crystals precipitate out of the metal flux. This process is analogous to dissolving sugar or salt into boiling water and then lowering the temperature until crystals come out of solution with the water.

For a more detailed explanation, we may consider our specific example of $BaFe_2As_2$. First it is necessary to consult a binary phase diagram. This diagram shows how much of the crystal constituents will dissolve into the metal flux at a given temperature. It is important to look for any binary compounds that exist among the crystal constituents at high temperatures because these may limit crystal growth.

Fig. 3 tells us that Arsenic will easily dissolve in Indium for temperatures greater that 500°C. Additionally, we note InAs is very stable (melting point at 942°C). We must hope that the crystals we are forming are more stable than InAs so that they preferentially form.

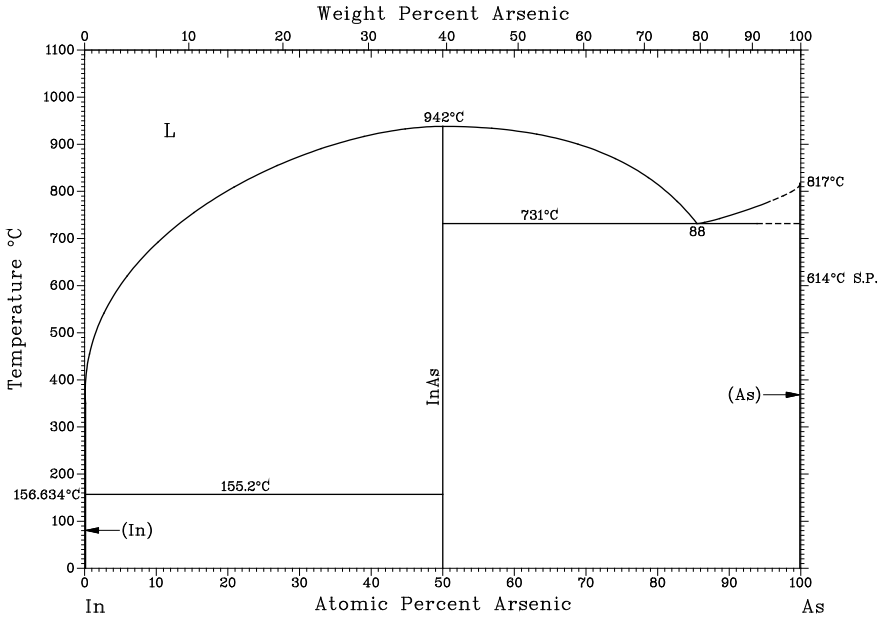

Fig. 3: This is a binary phase diagram for In and As. This plot indicates how much As will dissolve into In as a function of temperature. The melting point of the stable compound InAs is indicated. [4]

Once an adequate metal flux is found (for $BaFe_2As_2$ we were the first to use In) the elements' masses may be measured and placed in a sealed metal (Nb or Ta) crucible in preparation for placement in a tube furnace. Typically, we used 20-40 more moles of metal flux than crystal elements to allow the crystal elements to dissolve. The filled crucible is then subjected to a heating schedule in flowing argon to avoid oxidizing the crucible. A typical heating schedule is as follows. Start at room temperature. Then heat to 500°C at a rate of 75°C per hour. Then hold at 500°C for four hours. Then heat to 700°C at a rate of 75°C per hour. Then hold at 700°C for four hours. Then heat to 1000°C at a rate of 75°C per hour. Then hold at 1000°C for four hours. Then cool to 800°C at a rate of 2.5°C per hour. Then cool to 500°C at a rate of 5°C per hour. Then cool to room temperature at a rate of 75°C per hour.

After the crucible and its contents have made it through this cycle once (after about 1 week), we can remove the crucible. At this point, the $BaFe_2As_2$ crystals we seek are embedded in the solidified metal flux. The crystals are harvested by heating the crucible on a hot plate to a temperature above the melting point of the metal flux, which is below the melting point of the crystals we wish to harvest. The crystals are removed from the molten flux with tweezers and are then ready for measurement. Alternatively, the contents of the crucible may be centrifuged in a glass tube above ($T>T_{M,Flux}$) with a piece of glass wool at the bottom. The molten flux will pass through the glass wool but the solid crystals will be caught in the glass wool for easy harvesting.

As alluded to in the abstract, we are testing the relationship between I and V or measuring the resistance of this crystal at low temperatures. We, therefore, need to attach wires to the sample to apply currents and measure voltages. Looking through a microscope, we attach

four 0.002'' diameter platinum wires with silver epoxy to the edges of the crystal. An image of this configuration can be found in fig. 4.

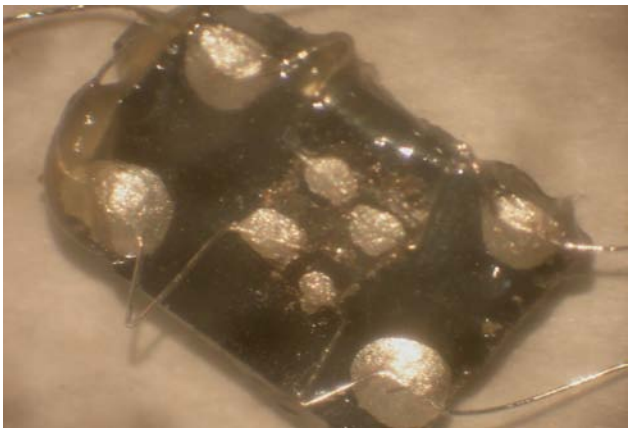

Fig. 4: A photograph of one of our $BaFe_2As_2$ crystals taken under a microscope. The crystal is at the center of the image and is mounted on silicon substrate to make it electrically isolated. Typical crystal dimensions are 1mm x 1mm x 0.1mm.

In fig. 5 the $BaFe_2As_2$ crystal is located in the center. Two of the wires are used to pass a dc current through the ab crystal plane and the other two are used to measure the voltage drop. Passing current through the crystal inevitably creates a heat gradient in the crystal, which creates a thermal voltage. In order to ignore this thermal voltage and concentrate on the current transport voltage, the current direction must be switched back and forth and the absolute value of the measured voltages must be averaged. Typically, each recorded voltage measurement is the average of 80-100 individual voltage measurements.

Once this wiring is completed, the crystal may be attached inside a sample probe in vacuum; the probe is then inserted into a liquid helium dewar. Temperatures as low as 4.2K are reached by filling the dewar with liquid ^{4}He. If the ^{4}He gas above the liquid in the dewar is pumped out, the crystal is cooled to about 1K.

Results and Discussion

Fig. 5 shows resistivity data for one of the $BaFe_2A_2$ crystals. The black circles are data taken before annealing. We are the first to observe a full superconducting resistive transition in undoped $BaFe_2A_2$. After taking these measurements, we annealed the crystal at 300°C for 2 hours under vacuum seal in Pyrex®. Then we measured the resistivity again and these data still exhibit a superconducting transition. These data (green triangles) are significant because they show that the superconducting transition has remained and, in fact, been made sharper. This is in

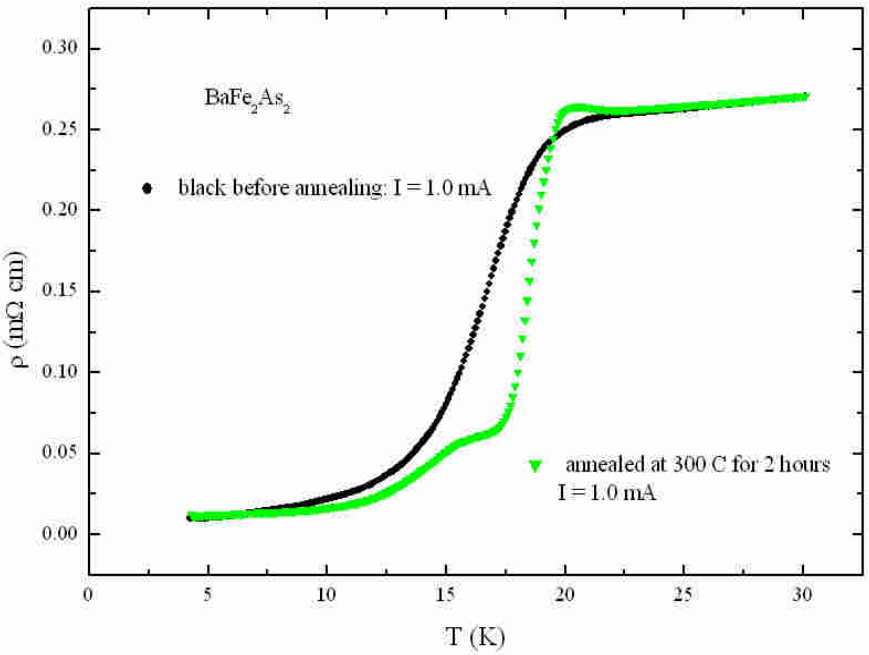

Fig 5. Data on a $BaFe_2As_2$ crystal before and after it was annealed. The black circles are data taken before annealing. The green triangles are data taken after annealing at 300°C for 2 hours.

contrast to Saha et al. [5] who found, in the similar compound $SrFe_2As_2$, that this annealing procedure destroyed the superconducting state. Saha et al. have posited that superconductivity in $SrFe_2As_2$ and perhaps other "122 structure" iron arsenic superconductors may be the result of crystallographic strain. The data presented in fig. 5 show that this is not consistent with our data in the compound $BaFe_2As_2$.

The interpretation, that fig. 5 counters the strain model in $BaFe_2As_2$, rests crucially on one as yet unstated assumption. It is assumed that nothing happened to alter the crystalline structure of the sample between annealing and cooling it back down for measurement. We did have instances when cooling other samples caused the sample to fracture. We know that the sample used for fig. 5 did not fracture but we cannot be sure, given this data, that cooling did not cause significant strain which, in turn, sharpened the superconducting transition in accordance with the strain model. We can only be sure that fig. 5 fails to verify the strain model but not that it is a counterexample.

Our next significant finding was that the superconducting transition is highly sensitive to the amount of current passed through the sample and that the upper critical field shared the anisotropy of the tetragonal crystal lattice for $BaFe_2As_2$. Fig. 6 shows three different samples of $BaFe_2As_2$, all of which have a noticeable superconducting transition. From fig. 6, it is easily seen that higher currents cause the resistive transition to be much broader. The resistivity for sample 1 with 1.5mA current does not even reach $\rho=0$ and, therefore, we can take 1.5mA as an estimate of the critical current (the current which destroys the superconducting state). This, given the dimensions of sample, is a critical current density of $1.5A/cm^2$. We can compare this number to those for bulk superconductors e.g., ~100 A/cm^2 in YBCO [6] and ~$10^4 A/cm^2$ MgB_2 [7]. This rather small critical current density and the fact that we did not observe a diamagnetic susceptibility signal in a squid magnetometer led us to consider that the superconductivity in these crystals was not a bulk property and may be filamentary or planar in nature.

Fig. 7 shows critical field anisotropies for our sample of $BaFe_2As_2$ and similar compounds tested by other researchers. Critical field anisotropies mean that the critical field for the superconductor has different values depending on whether the field is applied parallel to the

plane of the crystal (the ab plane) or perpendicular to the plane of the crystal (the c-axis). Since our critical fields exhibit the inherent anisotropy of the crystal, it is rendered less likely that the superconductivity arises from filaments, which may not share the anisotropy of the lattice. Additionally, we noticed after removing a couple of the micaceous layers from the top of a crystal that the transition became sharper and the temperature at which the resistivity went to zero increased by several degrees. Moreover, the inset of fig. 6 shows the change in the resistive transition before and after a crystal was broken parallel to the c-axis. The c dimension of the crystal was thus unchanged while the ab plane was changed. All these results lead us to favor planar superconductivity over filamentary superconductivity.

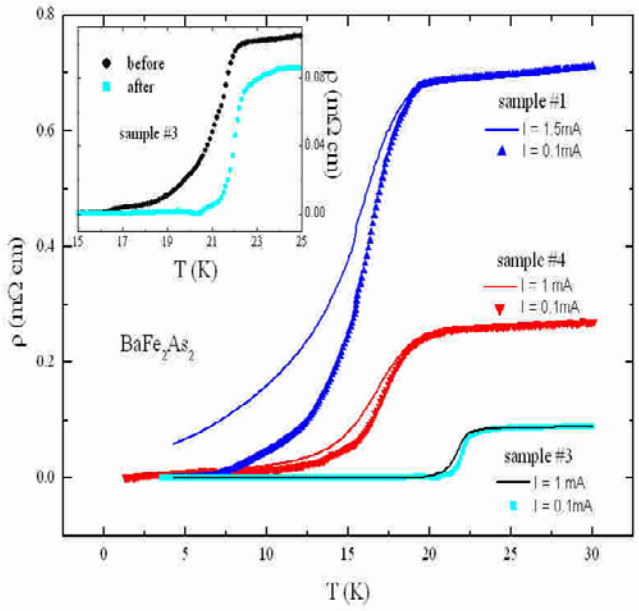

Fig. 6: Resistivity versus temperature curves for five different samples of $BaFe_2As_2$. Notably the resistivity with I=1.5mA does not go to zero, indicating, a critical current. The inset shows the resistivity of sample 3 before and after it was broken parallel to the c-axis.

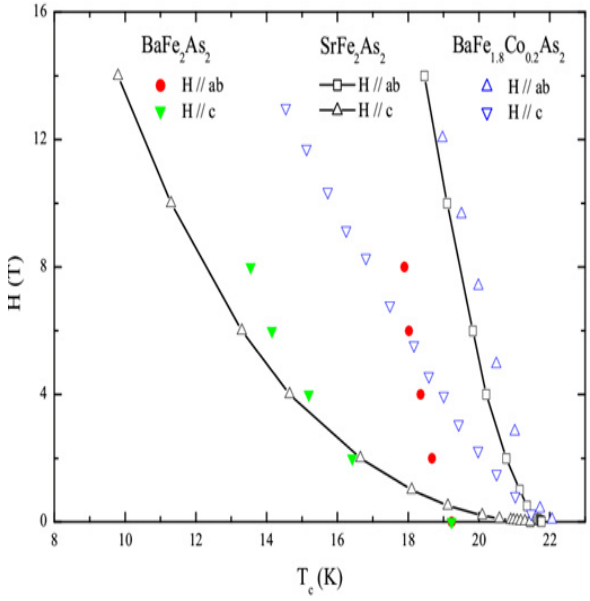

Fig. 7: Critical field data for $BaFe_2As_2$. Our field anisotropies are similar to those found in sample 1 $BaFe_{1.8}Co_{0.2}As_2$ by Kano [8] and those in $SrFe_2As_2$ by Saha et al. [5].

After we had this evidence, which suggests planar superconductivity, we decided to search for a Kosterlitz-Thouless transition, which is known to occur only for 2-D materials. Given the complex and subtle nature of a Kosterlitz-Thouless transition, theoretical introduction is given before diving into the data.

Introduction to Kosterlitz-Thouless Theory:

As materials are cooled to lower and lower temperatures the disordered states give way to well-ordered phases. At low temperatures, the ambient thermal energy is no longer great enough to dwarf the interaction energies between constituent parts of a system. As a result, long-range order (or quasi-long range order in the case of two dimensions) forms. A Kosterlitz-Thouless (KT) process is an example of such a phase transition.

The KT transition comes from considering the 2D XY model of solid-state physics. The 2D XY model consists of a system of spins located on a lattice (see fig. 8). We may associate

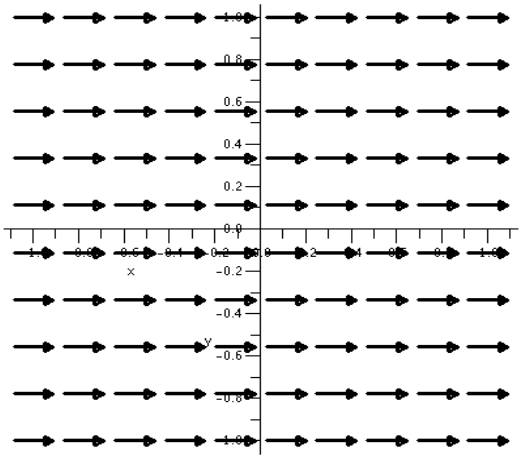

Fig. 8 An example of an XY model where all the spins are aligned. [9]

with this system an order parameter $\langle\psi\rangle = |\langle\psi\rangle|e^{i\theta}$. It has a magnitude, $|\langle\psi\rangle|$, and a phase, θ.

The mathematical model for the 2D XY model consists of the following Hamiltonian: $H = -J\sum_{\langle ij\rangle} \vec{s}_i \bullet \vec{s}_j = -J\sum_{\langle ij\rangle} \cos\left(\theta_i - \theta_j\right)$ [11]. In this formula J is a positive constant, the sum is over all nearest neighbors and θ_i represents the angle of the spin at site i. It is a well-known fact that

this 2D XY model possesses no long-range order phenomenon due to spin-wave excitations [11]. Nonetheless, Kosterlitz and Thouless were able to describe a non-traditional phase transition that corresponded to vortices. A vortex (as shown in fig. 9) is exhibited by a change of an integer multiple of 2π in the orientation of spins around a singularity. The spins can rotate clockwise (a vortex) or counterclockwise (an anti-vortex).

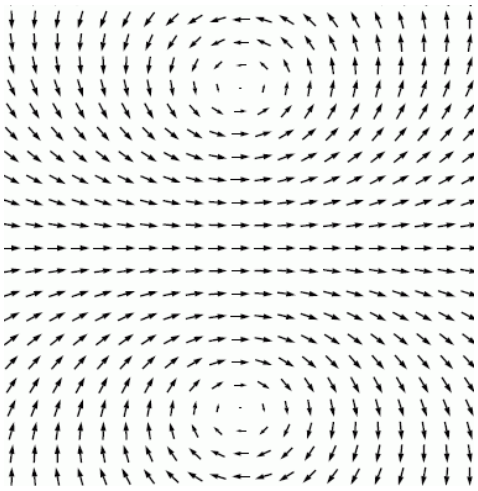

Fig. 9: A diagram of two vortices. Notice that the spins rotate about the center in two different senses. This is referred to as a vortex/anti-vortex pair. [10]

In order to continue the analysis of 2D XY model with vortices the Hamiltonian is approximated near a minimum in the following way: $H - E_0 \approx \frac{1}{2} J \sum_{\langle ij \rangle} \left(\theta_i - \theta_j\right)^2$ [11]. Using this approximation, we can say that in the 2D XY model the energy of these vortices is given by eq. 6 [11][12].

$$E = \pi k^2 \rho_s \ln\left(\frac{R}{a}\right) \tag{6}$$

Where R is the size of the system, a is the size of the core, ρ_s is the rigidity modulus, and k is called the winding number and its value indicates by which multiple of 2π the angles of the spins change around the center of the vortex (see fig. 9). Positive winding number is called a vortex and a negative winding number is called an anti-vortex. We can now look at the energy of two vortices. It will not be strictly additive because vortices interact with one another [12].

$$E = \pi\rho_s (k_1 + k_2)^2 \ln\left(\frac{R}{a}\right) + 2\pi\rho_s k_1 k_2 \ln\left(\frac{a}{r}\right) \quad (7)$$

Where r is the separation of the two vortices. We notice that if $\sum_i k_i = 0$ then the energy does not depend on the size of the system and thus the energy will not be arbitrarily large [11]. Thus the most energetically favorable state at very low temperatures will be one in which there are equal numbers of vortices and anti-vortices.

To continue this line of reasoning, we can consider the free energy, F=E-TS. The entropy of the system with a free vortex will be as shown in eq. 8 [11][12].

$$S = \ln\left(\left(\frac{R}{a}\right)^2\right) \quad (8)$$

Therefore, the free energy for a single vortex (with k=1) will take the form shown in eq. 9 [11][12].

$$F = \pi\rho_s \ln\left(\frac{R}{a}\right) - T\ln\left(\left(\frac{R}{a}\right)^2\right) = (\pi\rho_s - 2T)\ln\left(\frac{R}{a}\right) \quad (9)$$

From this equation we can see that there is a critical temperature, $T_{KT} = \frac{\pi\rho_s}{2}$ [11][12]. Below this temperature the energy term dominates and the free energy of the system is minimized by there being no free vortices. Above this temperature, the entropy term dominates and the free energy is minimized by the presence of vortices.

Eqs. 7 and 9 are the heart of the description of the Kosterlitz-Thouless process. Eq. 9 tells us that it is not energetically favorable to form individual vortices below the critical temperature. Eq. 7 tells us that to create a vortex-anti-vortex pair costs arbitrarily little energy. Moreover, from eq. 7 we can find the force,f_{21}, exerted by vortex 1 on vortex 2:

$f_{21} = -\nabla_2 E = 2\pi\rho_s k_1 k_2 \frac{(r_2 - r_1)}{|r_2 - r_1|^2}$ [12]. This shows that the force is attractive if the winding numbers are of opposite sign. Notice how this force law is the same as the force between two current-carrying wires placed at the center of the vortices, except with opposite sign [11]. Therefore, we can interpret this to mean that below the critical temperature our system can have vortex/anti-vortex pairs and above the critical temperature these pairs can be broken up to form free individual vortices. This is called a Kosterlitz-Thouless transition.

We have thus arrived at an understanding of a Kosterlitz-Thouless process but have yet to understand how it applies to superconductors. The arguments previously presented for the standard XY model will translate immediately to superconductors if the superconducting system is 2-D, has an order parameter with a magnitude and phase, and if vortices have the same logarithmic energy dependence.

From the BCS theory, the microscopic theory of superconductors, we know that there exists an energy gap for electron pairs (Cooper pairs). Moreover, this energy gap has a magnitude and a phase [13][14].

$$\Delta_{\mathbf{k}} \equiv |\Delta_{\mathbf{k}}| e^{(i(\phi_{1\mathbf{k}} - \phi_{2\mathbf{k}}))} \tag{10}$$

Where $\Delta_{\mathbf{k}}$ is the energy gap for an electron pair with momentum $\pm\mathbf{k}$ respectively. Therefore, the energy gap appears to be a prime candidate for an order parameter in superconductors. In fact, Gor'kov showed that the order parameter in the phenomenological Ginzburg-Landau theory for superconductors is actually proportional to the energy gap. [15][16]

Moreover, it can be shown using Ginzburg-Landau theory that an individual vortex has an energy given by eq. 11 [15][17].

$$E \approx \left(\frac{\Phi_0}{4\pi\lambda}\right)^2 \ln(k) \tag{11}$$

In eq. 11, Φ_0 is the flux quantum and can be replaced by $-\Phi_0$ to account for an anti-vortex. Thus Φ_0 is the analog of the k, the winding number, in the XY model. λ is the penetration depth, and κ is the Ginzburg-Landau parameter. κ is the ratio of two characteristic length scales of the system – λ and ξ, the coherence length – and can be arbitrarily large. Thus κ is an appropriate analog of (R/a) in the XY model. Additionally, the interaction between two vortices in a superconductor can be shown to be of the form given in eq. 12 [15][17].

$$E_{\text{int}} = \frac{\Phi_0\Phi_0}{8\pi\lambda^2} \ln\left(\frac{r}{\lambda}\right) \tag{12}$$

where r is the distance between the vortices. The analogies hold as previously stated.

We are led to conclude that a superconductor has an appropriate order parameter and vortex interactions of the same form as in the XY model. Therefore, we expect that, for a 2-D superconductor, a Kosterlitz-Thouless transition should be possible.

Extraction of the Kosterlitz-Thouless transition temperature, T_{KT}, is a challenging task, as the measured properties of the material do not exhibit sharp features at the transition. During my research program, I investigated no fewer than three separate methods to determine the transition temperature.

The first method investigated current-caused pair breaking. As previously mentioned, an electrical current will impart a force on a magnetic vortex; moreover, the force will be equal and opposite on each member of the vortex/anti-vortex pair. This means that the net force on the pair will be zero and thus it will not move, which maintains lossless conduction of electrons. However, the currents can impart a force so large as to break apart the vortex pairs. Then these individual vortices are moved by the electrical currents, which create a finite resistance. It can

be shown that a power law relationship between V and I holds near the Kosterlitz-Thouless transition in the limit that I goes to zero [22][18].

$$V \propto I^{\alpha(T)} \;\Leftrightarrow\; \log(V) = \alpha(T)\log(I) + const. \tag{13}$$

The power, $\alpha(T)$, in this relationship has the value 3 when $T=T_{KT}$. Therefore, a measurement of T_{KT} can be found by measuring currents and voltages across the crystal and finding the temperature at which V goes like I^3.

The second method of determining T_{KT} requires measuring the resistive transition into the superconducting state. In essence, this method measures temperature-caused pair breaking. The resistance near the resistive transition should have the following functional form.

$$R \sim e^{\frac{-const}{\sqrt{T-T_{KT}}}} \tag{14}$$

By fitting the resistivity curve to this functional form, we should be able to determine the constant T_{KT} [19].

The third method involved measuring the resistance of the crystal as an applied magnetic field was varied. Just as transport currents can break up vortex/anti-vortex pairs, so can a magnetic field. A magnetic field will place an equal and opposite force, $\vec{F} = -\nabla\left(\vec{m} \bullet \vec{B}\right)$, on the respective members of a vortex/anti-vortex pair. Measuring the resistivity of the sample as the magnetic field is varied can provide information about T_{KT}. With this method, we looked to satisfy the following equation [23][20]:

$$\left.\frac{d\ln\rho}{d\ln H}\right|_{T=T_{KT}} = 1 \tag{15}$$

Data and Analysis:

A partial set of data for current-caused pair breaking is presented below in fig. 10. Applying Kosterlitz-Thouless theory, as described in the introduction, tells us that the transition temperature, T_{KT}, is near 18K

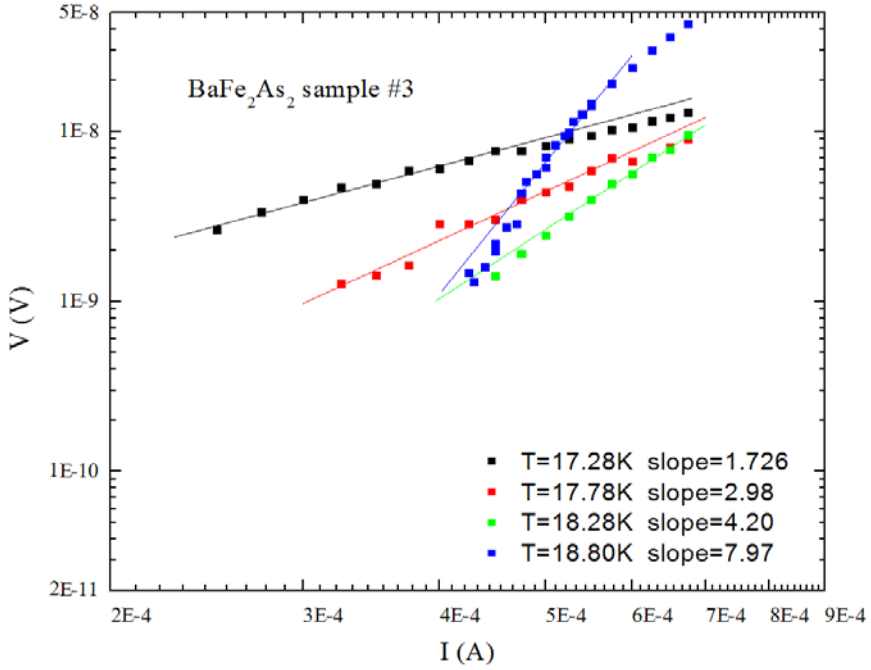

Fig. 10: VI curves for $BaFe_2As_2$. Fitted lines are shown for linear regions of the data as seen on a log-log plot. The data are labeled by the temperature at which they were taken and next to the temperature is the slope of the fitted line.

These voltage versus current measurements are experimentally difficult to obtain. To understand why we must remember that we only expect power law relationship between V and I (with power ~3) in the zero current limit. However, our instrumentation allowed us to only measure voltages on the order of nV. Moreover, once the current supplied reached ~0.8mA the power-law relationship disappeared. This explains the fitting region that is less than one decade of current. This small fitting region and apparent deviations from linearity on the log-log plot render this plot unconvincing. However, the fact that we do observe linear regions whose slopes pass through 3 and approach Ohmic behavior as the temperature is increased suggests to us that KT behavior may be present. To confirm this suggestion, we must corroborate with different measurement methods.

After the inconclusive KT results from measuring current-caused pair breaking, we attempted to measure temperature-caused pair break by fitting the resistive transition to the functional form given in eq. 14. In fig. 11, the fitted value for T_{KT} was 19.48K. We also noticed that the fit was significantly worsened if T_{KT} was changed by 0.1K, which indicates the error in this method. The agreement between measurement and theory is certainly better in this case. However, the large difference between the values of T_{KT} provided by these two methods gives us cause for pause.

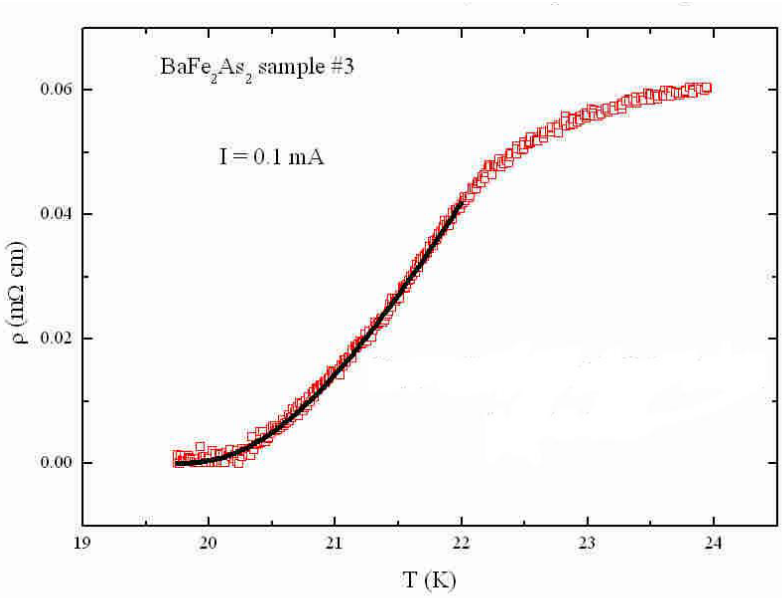

Fig. 11. A close-up of the resistive transition of $BaFe_2As_2$. The fitted line is of the form of eq. 14. The fit yields T_{KT}=19.48.

$$\rho(T) = 1.71715 \cdot e^{\frac{-5.89}{\sqrt{T-19.48}}}$$

Our third and final method used to find the KT transition was to measure the resistance of the sample as a function of magnetic field at a given temperature (magnetic field induced vortex pair breaking). The temperature at which eq. 15 is satisfied is T_{KT}. From fig. 12, we can see that T_{KT}=19.8 K ± 0.1K. This seems a reasonable value, the value is close to that obtained from the fit to eq. 14, and the slopes are monotonically decreasing with temperature, which we expect from the literature [20]. The agreement to within 0.4 K for T_{KT} is comparable to the 0.5K agreement found by Martin et al. [20], but they found the magnetic field calculation to provide

the lower approximation than the fit to eq. 14, which is opposite of our data. However, there are some subtleties with the data presented in fig. 12. Eq. 15 was derived under the assumption that the applied magnetic field was along the c-axis of the crystal. Our first measurement with magnetic field was parallel to the ab plane. This makes us wonder why we even saw Kosterlitz-Thouless behavior at all.

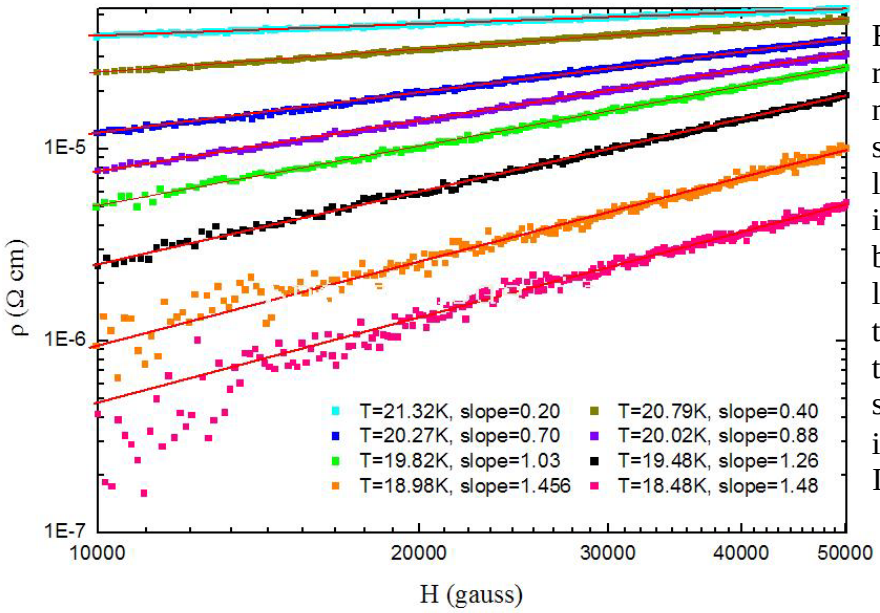

Fig. 12: Plots of the resistivity versus the applied magnetic field on a log-log scale. H || ab plane. Straight-line fits were made after the initial rise in the resistivity, between 1T and 5T. The legend indicates the temperature for each line and then a comma separates the slope of the line. This plot indicates $T_{KT} \approx 19.8K \pm 0.1K$. I = 0.1mA

Ando [21] also encountered this situation and postulated that the cause of KT behavior was the component of the magnetic field along the c-axis due to misalignment of the field in the ab plane. We assume Ando's explanation is correct, and we assume that there was a misalignment between the magnetic field and the ab plane by an angle θ. This means that the only component of our applied magnetic field that matters is Hsin(θ). Therefore we must adjust eq. 15 substituting our field parallel to the c-axis:

$$\left.\frac{d\ln(\rho)}{d\ln(H\sin(\theta))}\right|_{T=T_{KT}} = 1 \Leftrightarrow \left.\frac{d\ln(\rho)}{d\left[\ln(H)+\ln(\sin(\theta))\right]}\right|_{T=T_{KT}} = 1 \Leftrightarrow \left.\frac{d\ln(\rho)}{d\ln(H)}\right|_{T=T_{KT}} = 1 \qquad (16)$$

Since the end equation above is the same as eq. 15 we believe that our analysis is accurate. Nevertheless, these magnetic field measurements were taken over again with the field aligned with the c-axis to see if the value for T_{KT} changes. These data are displayed in fig. 13 and it too indicates that $T_{KT} \cong 19.7K \pm 0.1K$, therefore, we feel that Ando's explanation of the H||ab data is correct.

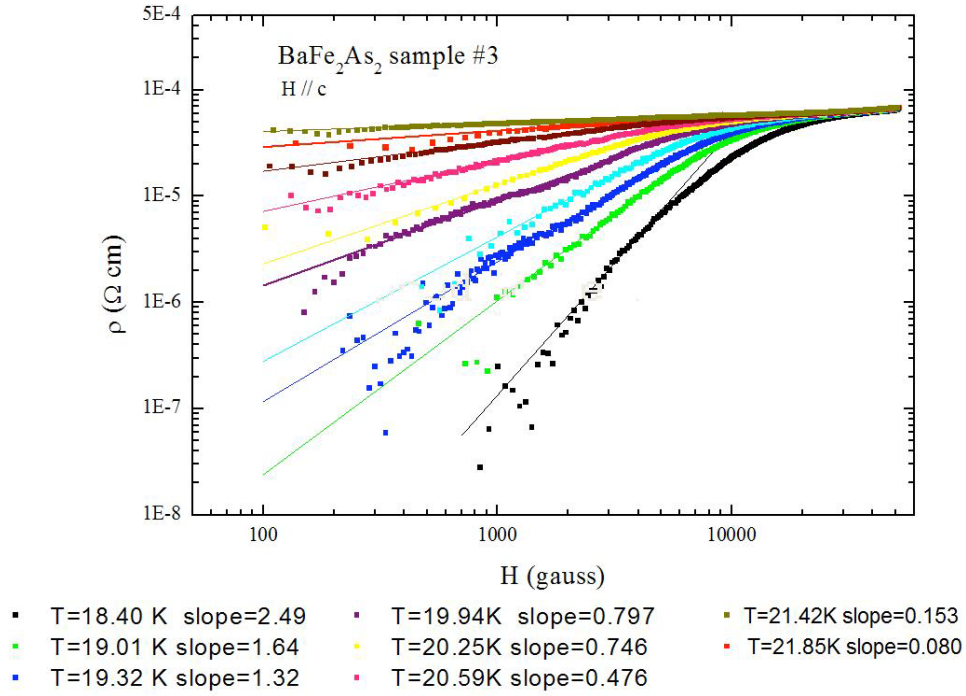

Fig. 13: Plots of the resistivity versus the magnetic field on a log-log plot. These plots are similar in appearance to those of Martin et al. [20]. I=0.1mA. This plot was provided by the Stewart research lab.

Early in the paper, we discussed at length the current dependence of the resistive transition. Therefore, the functional fit in fig. 11 also depends on the applied current. Moreover, it should be noted that the slopes in the resistivity vs. H plots also depend on the current applied to measure the resistivity (any finite current will cause additional vortex pair breaking). Therefore, while we are encouraged that the two values for T_{KT} agree, we must be careful. We

claim that we have observed a Kosterlitz-Thouless transition because the two independent methods agree; however, the exact value of T_{KT} determined by these methods will depend on the applied current.

Conclusions

We have repeatedly observed a superconducting transition in $BaFe_2As_2$. We have obtained data that fails to verify the model of strain-induced superconductivity for the compound $BaFe_2As_2$. This is because the superconductivity in our crystals did not vanish after annealing, which is in contrast to Saha et al. for undoped $SrFe_2As_2$ [5].

Two of three of methods for measuring the Kosterlitz-Thouless transition yielded consistent results for the transition temperature T_{KT}. The inconsistency of the VI curve measurements is the subject of further investigation.

The consistency of the temperature-induced pair breaking and magnetic field pair breaking methods (for the same applied current, I =0.1mA) give us confidence that this sample does undergo a Kosterlitz-Thouless transition with T_{KT} around 19.5K. However, the current dependence of these data indicates our value for T_{KT} is also current dependent. Finally, because we have observed a Kosterlitz-Thouless transition we can say that we have observed two-dimensional superconductivity in $BaFe_2As_2$.

Acknowledgements

I would like to thank the National Science Foundation for funding my research experience. I would like to thank the University of Florida for allowing me access to their facilities. I would like to thank Dr. Jungsoo Kim and Professor Stewart for their guidance, knowledge, and the independence they gave me in the lab and, more importantly, for granting me the ability to include the data obtained in their facilities in this thesis. Finally, I would like to thank Professor

Kurdak of the University of Michigan for agreeing to be my thesis chair and his thought-provoking suggestions.

References

1. Image taken from: http://reimer-hamburg.net/htc/pt3.html#Fig5
2. F. London and H. London, Proc. Roy. Soc. (London) **A149**, 71 (1935)
3. Image taken from: http://nd.edu/~vortex/research.html
4. Image taken from: Binary Alloy Phase Diagrams made by ASM International and NIST
5. S. R. Saha, N. P. Butch, K. Kirshenbaum, J. Paglione, Phys. Rev. Lett. **103**, 037005 (2009)
6. D. Kim, D. M. Kroeger, Journal of Materials Science **28**, 17 (1993) 4744-4748
7. C-Q. Jin, S-C. Li, J-L. Zhu, F-Y. Li, Z-X. Liu, and R-C. Yu, J. Mater. Res. **17**, 3 (2002) 525-527
8. M . Kano, Y. Kohama, D. Graf, F. F. Balakriev, A. S. Sefat, M. A. McGuire, B. C. Sales, D. Mandrus, and S. W. Tozer, arXiv 0904.1418v3 (2009)
9. Image taken from: http://www.math.rutgers.edu/~greenfie/mill_courses/math251/gifstuff/vf_horizconst1.gif
10. Image taken from: www.ibiblio.org/e-notes/Perc/xy.htm
11. J. M. Kosterlitz, D. J. Thouless, J. Phys. C **6**, 11(1972)
12. Chaikin, P.M., Lubensky, T.C. Principles of Condensed Matter Physics, (Cambridge University Press, Cambridge,1995)
13. J. Bardeen, L. N. Cooper, J. R. Schrieffer, Phys. Rev. **108**, 5 (1957)
14. Tilley, D.R., Tilley, J. Superfluidity and Superconductivity, 3rd ed. (Adam Hilger, New York, 1990)
15. Tinkham, M. Introduction to Superconductivity, (McGraw-Hill,1975)
16. L. P. Gor'kov, J. Exptl. Theor. Phys. (U.S.S.R.) **36**, 1918 (1959)
17. A. A. Abrikisov, J. Exptl. Theoret. Phys. (U.S.S.R.) **32**, 1442-1452 (1957)
18. A. M. Kadin, K. Epstein, A. M. Goldman, Phys. Rev. B **27**, 6691 (1983).
19. M. Wallin, H. Weber, Phys. Rev. B **51**, 6163 (1995).
20. S. Martin, A. T. Fiory, R. M. Fleming, G. P. Espinosa, A. S. Cooper, Phys. Rev. Lett. **62**, 677 (1989).
21. Y. Ando, N. Motohira, K. Kitazawa, J. Takeya, S. Akita, Phys. Rev. Lett. **67**, 2737 (1991)
22. Halperin, B.I. & Nelson, D.R. J. Low Temp. Phys. **36**, 599-616 (1979)
23. Minnhagen, P. Phys. Rev. B **23**, 5745-5761 (1981)